PESQUISA VETERINÁRIA BRASILEIRA
Brazilian Journal of Veterinary Research
ISSN 0100-736X (Print)
ISSN 1678-5150 (Online)

Pesq. Vet. Bras. 44:e07447, 2024
DOI: 10.1590/1678-5150-PVB-7447

Original Article
Small Animal Diseases

Neurocryptococcosis in dogs and cats: Anatomopathological and fungal morphological aspects in a case series[1]

Miguel D. Oliveira[2], Mariana M. Flores[3], Alexandre Mazzanti[4], Rafael A. Fighera[3] and Glaucia D. Kommers[3]*

ABSTRACT.- Oliveira M.D., Flores M.M., Mazzanti A., Fighera R.A & Kommers G.D. 2024. **Neurocryptococcosis in dogs and cats: Anatomopathological and fungal morphological aspects in a case series.** *Pesquisa Veterinária Brasileira 44:e07447, 2024.* Laboratório de Patologia Veterinária, Departamento de Patologia, Centro de Ciências da Saúde, Universidade Federal de Santa Maria, Av. Roraima 1000, Cidade Universitária, Bairro Camobi, Santa Maria, RS 97105-900, Brazil. E-mail: glaukommers@yahoo.com

Cryptococcosis is a fungal infection that commonly affects dogs and cats, often manifesting with neurological involvement. This study investigated the neuropathological characteristics of cryptococcosis in nine cats and two dogs submitted to necropsy through gross pathology and histopathological analysis. Clinical history, lesion location, fungal burden, type and intensity of inflammatory infiltrate, lesions in nervous parenchyma, and morphological characteristics of yeast cells were evaluated. Additionally, fungal morphological criteria, such as capsule and yeast wall thickness and budding frequency, were analyzed in each neurolocation. The Alcian blue stain method was utilized to enhance the visualization of yeasts. Debilitating and/or immunosuppressive conditions were described in five cases. Two cats were recently adopted from the streets, and one cat was treated with corticosteroids. One dog had severe cachexia and generalized weakness, and another dog had leukopenia with left shift. Only six cases (54%) had neurological signs. Gross central nervous system (CNS) lesions were found in five cases and appeared as irregular, friable, soft, gelatinous, and grayish masses with distinct borders. The telencephalic cortex and the cerebellum were the most frequently affected CNS locations observed in all cases. The first exhibited a higher fungal burden and a milder inflammatory response than other neurolocations. The cerebellum was also affected in all cases but showed a slightly higher inflammatory response and a lower fungal burden compared to the telencephalic cortices. Additionally, lung involvement was observed in all cases as well. The inflammatory intensity associated with the yeasts in the CNS was predominantly mild to moderate, being severe only in two cases, and the fungal burden was more often moderate or severe, being mild in only two cases. The observed heterogeneity in the inflammatory response and fungal burden reveals the complex nature of this infection. Other affected nervous tissues were the optic nerve, the spinal cord nerve roots and the ganglia, mostly in cats. In conclusion, our study shows the neuropathological features of cryptococcosis in a case series in cats and dogs, emphasizing the importance of considering specific neurolocations to diagnose this fungal infection and contributing to a better understanding of the simultaneous involvement of the respiratory and nervous systems.

INDEX TERMS: Cryptococcosis, histopathology, neurolocation, nervous system, dogs, cats.

[1] Received on April 4, 2024.
Accepted for publication on May 22, 2024.
Part of Master's Thesis of the first author.

[2] Programa de Pós-Graduação em Medicina Veterinária, Universidade Federal de Santa Maria (UFSM), Av. Roraima 1000, Cidade Universitária, Bairro Camobi, Santa Maria, RS 97105-900, Brazil.

[3] Laboratório de Patologia Veterinária, Departamento de Patologia, Centro de Ciências da Saúde, Universidade Federal de Santa Maria (UFSM), Av. Roraima 1000, Cidade Universitária, Bairro Camobi, Santa Maria, RS 97105-900, Brazil. *Corresponding author: glaukommers@yahoo.com

[4] Departamento de Clínica de Pequenos Animais, Centro de Ciências Rurais, Universidade Federal de Santa Maria (UFSM), Av. Roraima 1000, Cidade Universitária, Bairro Camobi, Santa Maria, RS 97105-900, Brazil.

RESUMO. [**Neurocriptococose em cães e gatos: aspectos anatomopatológicos e morfológicos fúngicos em uma série de casos.**] A criptococose é uma infecção fúngica que comumente afeta cães e gatos, muitas vezes se manifestando com envolvimento neurológico. Neste estudo, foram investigadas as características neuropatológicas da criptococose em nove gatos e dois cães submetidos à necropsia, por meio da análise macroscópica e histopatológica. Foi avaliada a história clínica, localização das lesões, carga fúngica, tipo e intensidade do infiltrado inflamatório, lesões no parênquima nervoso e características morfológicas das células de levedura. Além disso, critérios morfológicos fúngicos, como espessura da cápsula e parede da levedura e frequência de brotamento, foram analisados em cada neurolocalização. Para aprimorar a visualização das leveduras, foi utilizada a técnica de coloração de azul alciano. Condições debilitantes e/ou imunossupressoras foram detectadas em cinco casos. Condições debilitantes e/ou imunossupressoras foram descritas em cinco casos. Dois gatos foram recentemente adotados das ruas e um gato foi tratado com corticosteroides. Um cão apresentava caquexia grave e fraqueza generalizada e outro cão apresentava leucopenia com desvio à esquerda. Apenas seis casos (54%) apresentaram sinais neurológicos. Lesões macroscópicas no sistema nervoso central (SNC) foram encontradas em cinco casos, aparecendo como massas irregulares, friáveis, moles, gelatinosas e acinzentadas, com bordas distintas. O córtex telencefálico e o cerebelo foram as localizações do SNC mais frequentemente afetadas, observadas em todos os casos. O córtex apresentou uma carga fúngica mais elevada e uma resposta inflamatória mais branda em comparação com outras neurolocalizações. O cerebelo também foi afetado em todos os casos, apresentando uma resposta inflamatória um pouco mais elevada e carga fúngica mais baixa do que o córtex telencefálico. Além disso, o envolvimento pulmonar também foi observado em todos os casos. A intensidade inflamatória associada às leveduras no SNC, foi predominantemente leve a moderada, sendo grave apenas em dois casos, e a carga fúngica foi mais frequentemente moderada ou grave, sendo leve em apenas dois casos. A heterogeneidade observada na resposta inflamatória e carga fúngica revela a natureza complexa dessa infecção. Outros tecidos nervosos afetados foram o nervo óptico e as raízes e gânglios nervosos da medula espinhal, principalmente em gatos. Em conclusão, nosso estudo mostra as características neuropatológicas da criptococose em uma série de casos em gatos e cães, enfatizando a importância de considerar neurolocalizações específicas para o diagnóstico dessa infecção fúngica. Além disso, contribui para uma melhor compreensão do envolvimento simultâneo dos sistemas respiratório e nervoso.

TERMOS DE INDEXAÇÃO: Criptococose, histopatologia, neurolocalização, sistema nervoso, caninos, felinos.

INTRODUCTION

The prevalence of fungal diseases in humans and domestic animals has been commonly reported, possibly due to the rise in immune-suppressive therapies and climate change (Guarner & Brandt 2011, Seyedmousavi 2018). Among the most significant systemic mycoses, cryptococcosis has emerged as a fungal infection with significant lethality and morbidity. Typically presenting as meningoencephalitis, it is often secondary to cutaneous or pulmonary processes and can occur in both immunocompetent and immunocompromised individuals (Lacaz et al. 2002, Eghwrudjakpor & Allison 2009).

Cryptococcus spp. are encapsulated dimorphic yeasts responsible for causing infections worldwide in various species, including humans, domestic, wild, and laboratory animals. In cats, it is the most common systemic mycotic disease. The pathogenic species of *Cryptococcus* most often reported are *C. neoformans* and *C. gattii* (Caswell & Williams 2007). *Cryptococcus neoformans* is currently divided into two varieties: *C. neoformans* var. *grubii* and *C. neoformans* var. *neoformans* (Greene 2012). It has been proposed the separation of *C. neoformans* var. *grubii* and *C. neoformans* var. *neoformans* as separate species (*C. neoformans* and *C. deneoformans*, respectively), as well as the recognition of five species within *C. gattii* (namely *C. gattii, C. bacillisporus, C. deuterogattii, C. tetragattii, C. decagattii*) and four hybrid species (Hagen et al. 2015). This fungus is distinctive among all pathogenic fungi in domestic species because it has a mucopolysaccharide capsule that acts as a virulence factor, impairing phagocytosis and the migration of leukocytes. It also inhibits the synthesis of pro-inflammatory cytokines, inactivates the complement system, and can suppress T-cell responses (Buchanan & Murphy 1998, Bovers et al. 2008, Sykes & Malik 2012). The host's inflammatory response is variable and usually minimal, consisting of macrophages, lymphocytes, and plasma cells (Summers 1995, Steenbergen & Casadevall 2003).

Cryptococcosis can either be localized or spread throughout the body. There is tropism in the respiratory system, particularly the nasal cavity and the central nervous system (CNS) (Sykes & Malik 2012). The neurotropism is explained by the yeast's production of an enzyme called phenoloxidase, which allows them to synthesize melanin from diphenolic compounds, such as catecholamines (Williamson et al. 1998, Baker et al. 2022). The transmission of cryptococcal infections probably occurs through inhalation of dust contaminated by viable yeasts, leading to infection of the upper respiratory tract and lungs, followed by secondary hematogenous spread to the CNS, eyes, skin, and other organs (Faria & Xavier 2009). Yeasts may also reach the encephalon by extension, from a nasal lesion, either through the cribriform plate or the optic nerves (Lester et al. 2004, Malik et al. 2006). It is described that cryptococcal organisms were consistently identified in the cerebrospinal fluid analysis in samples collected from cisternal and lumbar regions of animals exhibiting signs of diffuse CNS disease, indicating the potential dissemination of yeasts through the cerebrospinal fluid. The presence of yeasts inside the central canal of the spinal cord, described by these authors in histopathological examination, also corroborates this theory (Sykes et al. 2010).

Important aspects of the cryptococcosis in the nervous system (neurocryptococcosis) are well described in humans, including the most affected neurolocations, type and intensity of inflammation, how yeasts enter the CNS, and the morphological features that are considered virulence factors (Chang et al. 2004, Charlier et al. 2005, Guevara-Campos et al. 2009, Pinto 2010). However, this data is still scarce in animals, with a few studies detailing the involvement of the nervous system (Sykes et al. 2010, Trivedi et al. 2011). The present retrospective study aimed to provide a detailed description of the infection by *Cryptococcus* spp. in 11 cases (nine cats and two dogs) by characterizing the neurolocation of the lesions, the inflammatory response and intensity, and the variations in yeast's morphology.

MATERIALS AND METHODS

Ethical approval. In this study, we did not perform any animal experiments. All the data were obtained from the archives of necropsy reports. All the samples (paraffinized tissues) used in this work came from the archives of the diagnostic routine of the veterinary pathology laboratory.

A total of 11 animals retrospectively studied were included in the case series. Consisting of nine cats (Cases 1 to 9) and two dogs (Cases 10 and 11), all submitted to necropsy and diagnosed with cryptococcosis affecting the nervous system (NS). Necropsy reports were selected and reviewed.

Information regarding the animal profile, such as species, breed, sex, and age, was collected from pathology reports. The clinical history of each animal was also reviewed, from which data regarding clinical signs, potential predisposing factors, concomitant diseases, treatment, and clinical progression were extracted. Gross lesion descriptions from the reports were also reviewed, and archived photographs were reassessed when available.

Paraffin blocks were collected from the laboratory archive and sectioned for histology using routine methods. Two slides were prepared from each block, one stained by hematoxylin-eosin (HE), one stained by Alcian blue pH 2.5 (and counter-stained by HE). The slides were then analyzed under light microscopy. This histomorphological study focused on the NS. Additionally, lung and eye lesions (focusing on the optic nerve) were also reevaluated. Involvement of other organs/tissues was only noted.

On histopathological reevaluation of the NS lesions, the following criteria were observed: a) locations of the lesions in the CNS anatomical regions (encephalon – frontal, parietal, and occipital cortex, basal ganglia, thalamus, hippocampus, mesencephalon, cerebellum, and pons; and spinal cord – cervical, thoracic, and lumbar segments), considering the availability and identification of the paraffin blocks of each case; b) location of the lesions in the CNS histological regions (meninges, neuropile, perivascular spaces, choroid plexus and vascular wall; c) lesions in the peripheral nervous system (when tissues were available, including the optic nerve, spinal nerve roots and ganglia); d) type and intensity of inflammatory infiltrate; e) fungal burden and vascular embolism; and f) morphological characteristics of the yeasts (cell shape, cell wall thickness, and capsule thickness).

Inflammatory response and fungal burden were subjectively categorized as severe = 3, moderate = 2, mild = 1, or absent = 0. The number of cases affected for each specific neurolocation was considered, and the score of each case for inflammatory response and fungal burden was added and divided by the number of individuals with involvement in each neurolocation, resulting in an average value of each coefficient for a better comparison between neurolocation. Morphological criteria, such as capsule and yeast wall thickness, were also analyzed and classified as decreased, regular, or increased (subjectively compared to the parameters of Galiza et al. (2014). The frequency of budding was also considered and subjectively classified as high, regular, or low.

RESULTS

Animals and clinical aspects

Eight animals were mixed-breed, and three were purebred (one dog – Labrador Retriever and two cats – Siamese and Persian). Among the dogs were one male and one female, aged one year and 10 months old, respectively. Among cats, there were five males and four females, age ranging from one to 10 years old. The average age was four years and two months.

Only three cases (27%) were clinically diagnosed with cryptococcosis. A complete neurological examination was performed on 27% of the animals (two cats and one dog). Clinical signs are shown in Table 1. Six animals (54%) were reported to have neurological signs (four cats and two dogs), among which blindness (Cases 10 and 11) and head tilt (Cases 6 and 8) were the most common signs. Respiratory signs were reported in four cases (Cases 1, 6, 7 and 9). One case (Case 1) showed a diffuse interstitial pattern on the thoracic X-ray (reported as compatible with viral pneumonia or neoplasm). Cutaneous lesions were present in three cases (27%), seen only in cats (Cases 2, 3 and 9) and described as multiple, raised, gelatinous and occasionally ulcerated nodules; they were white and amorphous on the cut surface, draining content resembling pus. Predominantly, these lesions were found on the head, thoracic and abdominal regions, and limbs.

Debilitating and/or immunosuppressive conditions were described in five cases: two cats with a history of being recently adopted from the streets (Cases 2 and 9); a cat that

Table 1. Neurological and other clinical signs in each case (n=11)

Case	Neurological signs	Other clinical signs
1	NR	Cough
2	NR	Cutaneous lesions
3	NR	Cutaneous lesions
4	NR	Anorexia, apathy, and weakness
5	Syncope	NR
6	Head tilt	Dyspnea
7	Somnolence, diminished postural reactions, cerebellar and vestibular ataxia, and negative patellar reflex	Dyspnea
8	Head tilt and paraplegia	NR
9	NR	Apathy, weakness, dyspnea, and cutaneous lesions
10*	Blindness and incoordination	NR
11*	Blindness and pain (upon epaxial palpation throughout the vertebral column)	Apathy and weakness

NR = not reported; * cases of dogs.

had previous treatment with corticosteroids (Case 6); one dog that presented severe cachexia and generalized weakness (Case 11), and a dog with clinical history of leukopenia with left shift (Case 10). Cryptococcosis treatment (specific drug not informed) was reported only in one cat (Case 3).

Gross pathology

Gross lesions in the CNS were documented in five cases (Cases 6, 7, 8, 9 and 11), observed most frequently in the piriform lobe (Fig.1) (Cases 7, 8 and 9) and on the frontal lobe, parietal lobe, occipital lobe, brainstem, hippocampus, cerebellum (Fig.2), and spinal cord (one case each). One dog (Case 11) had lesions in the spinal cord, located in the cervical and lumbosacral regions (Fig.3). In two cases with ocular involvement (Cat 8 and Dog 11), there was swelling of the extracranial portion of the optic nerve (Fig.4).

Cryptococcal lesions appeared as irregular, friable, soft, gelatinous, and grayish masses with distinct borders, ranging in size from 0.1 to 2cm, seen either as exophytic nodules on the surface of the brain or as nodules expanding the neuroparenchyma, seen on the cut surface (Fig.1). They occasionally caused asymmetry of the piriform lobes, with enlargement of the right side (Cases 8 and 9). Congestion or opacity of the leptomeninges (Fig.2) and focal hemorrhage in the frontal and parietal lobes were also described (one case each). In the spinal cord, exophytic nodules in the subdural space, as well as thickening of the nerve roots (Fig.3), were also observed.

Histopathology

Among the available histological sections, the telencephalic cortex was one of the most affected CNS locations, seen in all

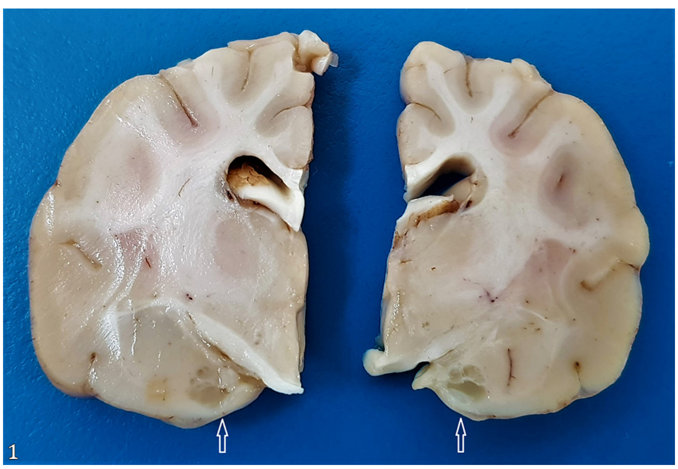

Fig.1. Piriform lobes with friable, soft, round, gelatinous, and grayish nodules expanding the parenchyma, ranging from 0.1 to 2cm (arrows). Neurocryptococcosis, cut surface of the telencephalic cortex, cat, Case 7.

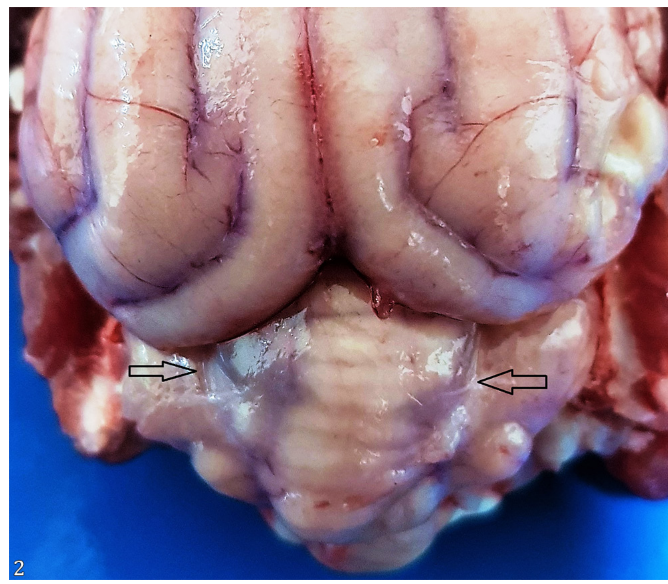

Fig.2. Soft, round, gelatinous, and grayish nodules expanding the meninges and causing meningeal opacity, ranging from 0.1 to 1cm (arrows). Neurocryptococcosis, cerebellum, cat, Case 6.

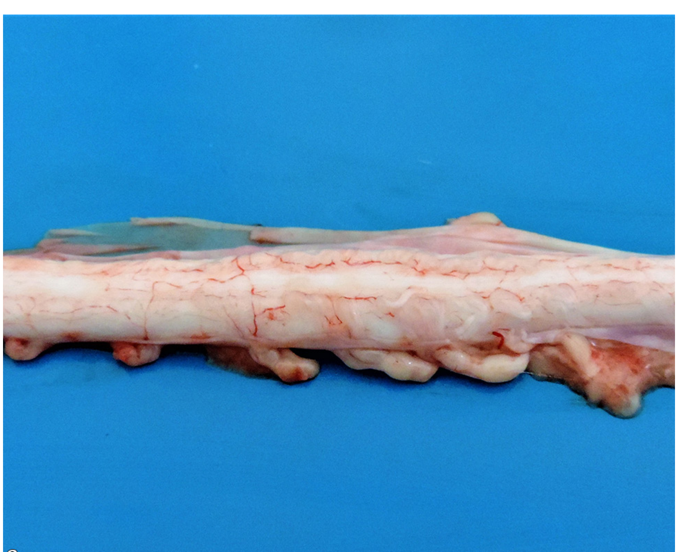

Fig.3. Enlargement of the nerve roots. Neurocryptococcosis, spinal cord (lumbar region), dog, Case 11.

Fig.4. Bilateral swelling of the extracranial portion of the optic nerve Neurocryptococcosis, eye, dog, Case 11.

cases, with lesser inflammatory response and higher fungal burden (on average). The exact distribution of the lesions among the cortical sections was identified in nine cases. The frontal cortex was involved in four cases, the parietal cortex in six, and the occipital cortex in five. In two cases, the specific location among the telencephalic cortices was not informed. Cerebellum involvement was also seen in all cases. However, compared to the telencephalic cortex, it exhibited a slightly milder inflammatory response and a significantly lower fungal burden. The distribution of the lesions, the inflammatory response, and the fungal burden on the nervous system are summarized in Table 2.

Yeasts were observed infiltrating the neuropil in eight cases (all except Cases 5, 9 and 10), in the following locations: telencephalic cortex in seven cases (77.7%), cerebellum in eight cases (88.8%), thalamus, hippocampus, pons and mesencephalon in one case each (11.1%). A predilection for either white or gray matter was not identified. In the cerebellum, two cases had yeasts infiltrating all layers (molecular and granular layers and white matter). They were present only within the molecular and granular layers in three cases. On encephalon sections, lesions in the neuropil were rarely observed, seen as a slight vacuolization of the parenchyma (Case 2 and 6), usually within areas of the interface between gray and white matter. In some areas, usually on the telencephalic cortex and sometimes on the cerebellum, the yeast clusters distended the sub-arachnoid space, causing compression of the subjacent parenchyma (Case 6).

Overall, there was a predominance of histiocytic inflammation. The intensity of the inflammatory response and fungal burden are shown in Figure 5-8 and Table 3. Cases were classified according to the predominant pattern observed; however, there was marked variation in both fungal burden and the type and intensity of inflammation within the same cases and, often, within the same histological section.

The inflammatory response was usually mild to absent in fields with higher fungal burden, wherein yeasts often formed aggregates with a predominance of foamy macrophages admixed with few neutrophils (Fig.5 and 8). Yeasts were predominantly seen around blood vessels, expanding the Virchow-Robin spaces (Fig.9). Sometimes yeast's clusters formed macroscopically visible nodules (Cases 2, 4, 6, 7 and 11), in the meninges and neuropil (Fig.10-11). These lesions were associated with thick and broad capsuled yeasts and were most common in cats. Narrow-based budding was most frequently observed within these areas and sometimes around the choroid plexus (Fig.12). By comparing the histopathological findings to the gross lesions, measuring the extent of space occupied by the aggregated yeasts in the subarachnoid space and within the neuropil, by high-power field counting (400x), it was observed that for a lesion to be noticeable on gross examination, it was necessary to have a minimum extension of 1mm.

Areas with lower fungal burden had a predominance of granulomatous inflammation with a variable amount of multinucleated giant cells (Fig.6), and sometimes, in these areas, there was a lymphoplasmacytic inflammation with scarce neutrophils. These lesions were frequent in Cases 10

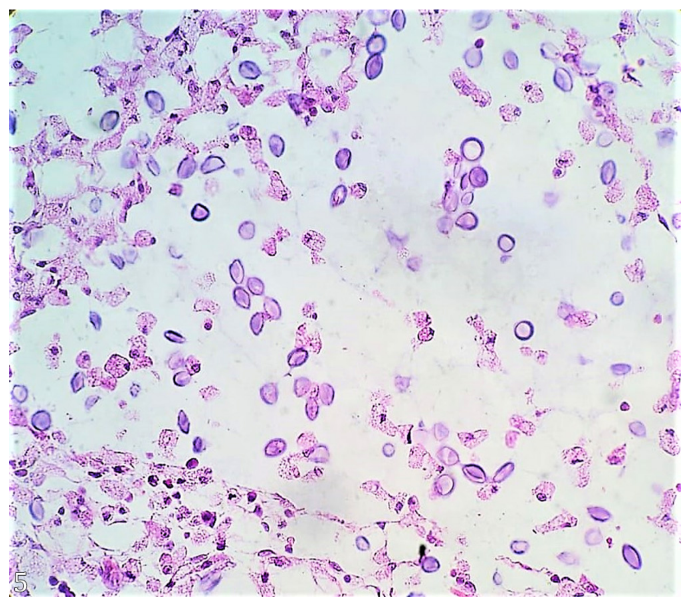

Fig.5. Aggregated yeasts surrounded by mild inflammation; predominance of foamy macrophages, fewer lymphocytes and plasma cells; severe fungal burden. Neurocryptococcosis, telencephalic cortex (meninges), cat, Case 7. HE, obj.40x.

Table 2. Inflammatory intensity and fungal burden average score in the central nervous system (CNS) of each neurolocalization (n=11)

Nervous system location	Cases (n)*	Inflammatory response (average value)**	Fungal burden (average value)**
Telencephalic cortex	11 (11)	1.36	2.27
Basal ganglia	1 (1)	3	1
Thalamus and hippocampus	8 (9)	1.11	1.88
Mesencephalon	3 (4)	0.75	2
Cerebellum	11 (11)	1.45	1.9
Choroid plexus	3 (3)	2.25	1
Pons	5 (6)	1	1.66
Spinal cord (cervical, thoracic and lumbosacral)/nerve roots/para-vertebral ganglia	4 (4)	0.75	2
Optic nerve	2 (2)	1.5	2.5

* The number of cases with each specifically affected neurolocalization was considered among the available paraffin blocks (n), **The score of each case for inflammatory response and fungal burden was added and divided by the number of individuals with involvement of each neurolocalization, resulting in an average value of each coefficient.

and 11 (both dogs). Two cases (Case 5 and 6) were distinctive for a severe perivascular lymphoplasmacytic inflammation expanding the Virchow-Robin spaces, forming up to 18 layers of inflammatory cells (Fig.13); rare yeasts were seen within these areas. In Case 6, there was also lymphoplasmacytic choroid plexitis and meningitis with rare yeasts associated with these lesions.

Spinal cord involvement was observed in one dog (Case 11) and three cats (Cases 7, 8 and 9). Inflammatory infiltrate mainly consisted of lymphocytes and plasma cells, with foamy macrophages in fewer amounts and rare neutrophils in this organ. In all cases with spinal cord involvement, yeasts were on the subdural space, sometimes infiltrating the leptomeninges in all regions (cervical, thoracic and lumbosacral), sometimes forming macroscopically visible nodules (Case 11).

Yeasts were not seen infiltrating the neuropil on the spinal cord. However, sometimes, there was compression of the underlying parenchyma where aggregated yeasts were observed, wherein a slight presence of multifocal axonal degeneration was seen, characterized by swollen axons (spheroids), digestion chambers and fragmented myelin sheaths in the white matter. Nerve root invasion was seen

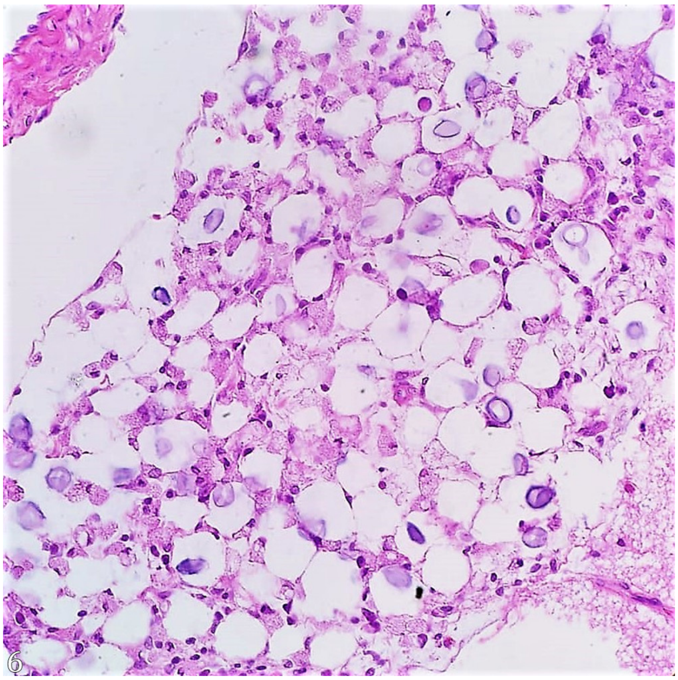

Fig.6. Aggregated to individualized yeasts, surrounded by moderate inflammation; predominance of foamy macrophages, slight increase in the number of lymphocytes and plasma cells; moderate fungal burden. Neurocryptococcosis, telencephalic cortex (meninges), cat, Case 4. HE, obj.40x.

Table 3. Intensity of inflammation and fungal burden for each case (n=11)

Case	Inflammatory intensity	Fungal burden
1	Moderate	Severe
2	Mild	Severe
3	Mild	Severe
4	Moderate	Moderate
5	Severe	Mild
6	Moderate	Severe
7	Mild	Severe
8	Moderate	Severe
9	Severe	Mild
10*	Moderate	Moderate
11*	Moderate	Moderate

* Cases of dogs.

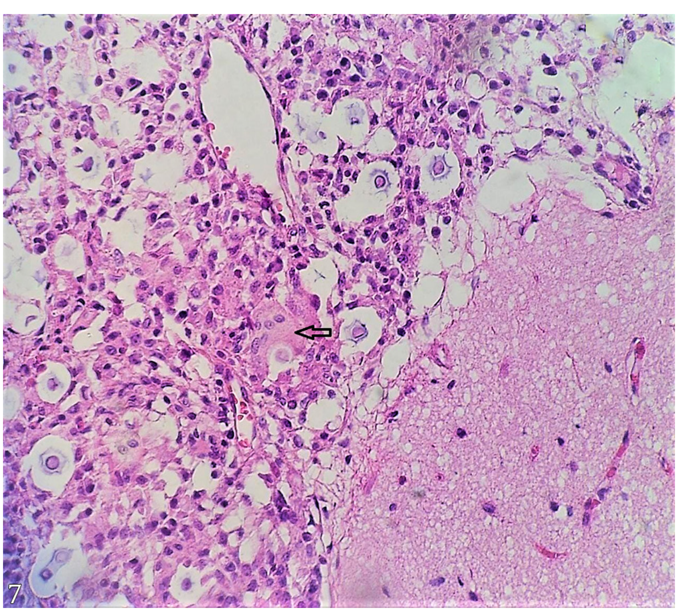

Fig.7. Individualized and interspersed yeasts by severe inflammation; predominance of lymphocytes and plasma cells, with fewer macrophages; mild fungal burden. Indicates multinucleated giant cell engulfing a yeast (arrow). Neurocryptococcosis, telencephalic cortex (meninges), dog, Case 1. HE, obj.40x.

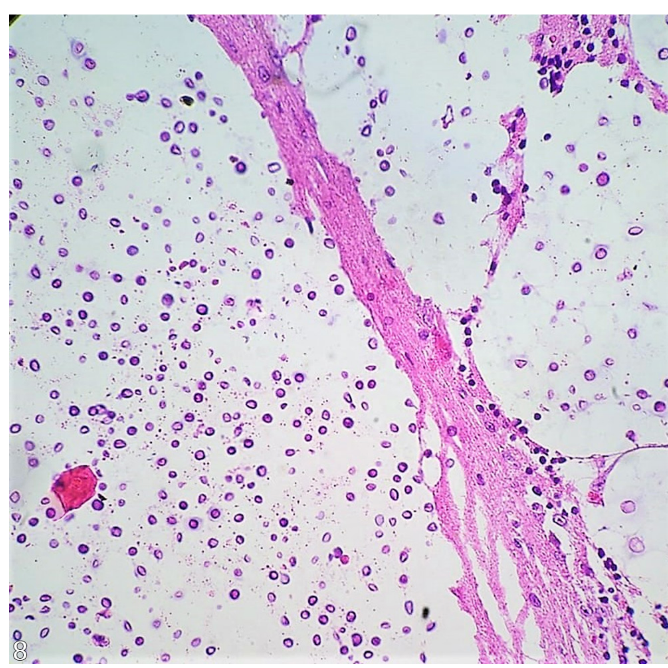

Fig.8. Aggregated yeasts surrounded by no inflammation; severe fungal burden. Neurocryptococcosis, cerebellum (meninges), cat, Case 2. HE, obj.20x.

in Cases 7 and 11 (Fig.14), sometimes in the epidural space around them, causing the enlargement of the nerve roots described. The paravertebral ganglia were affected in Case 7, with yeasts invading and partially replacing the nervous tissue. Two cases (Cases 7 and 11) had ocular involvement, with partial to total replacement of the optic nerve by yeasts (Fig.15).

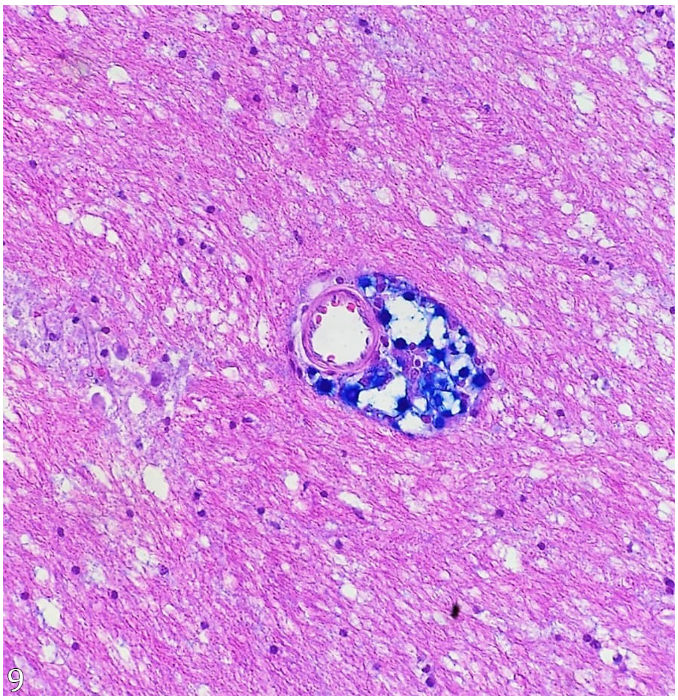

Fig.9. Blue-stained yeasts around blood vessels in the neuropil, expanding the Virchow-Robin spaces. Neurocryptococcosis, telencephalic cortex (white matter), cat, Case 3. Alcian blue, obj.40x.

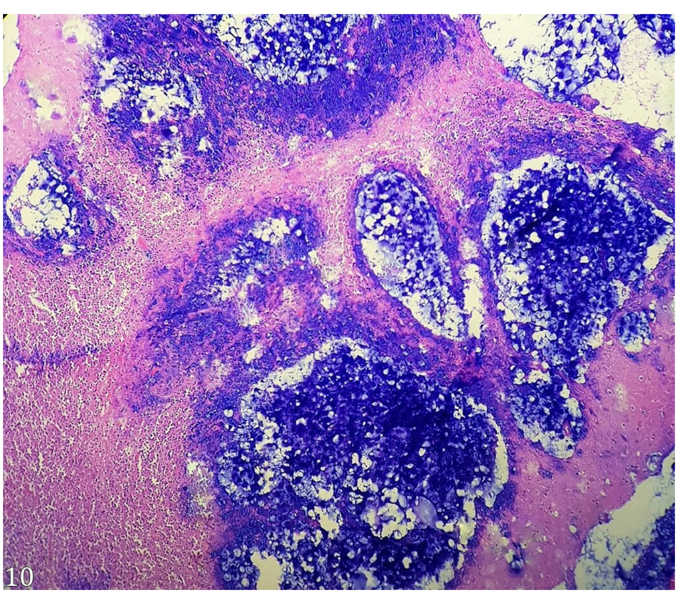

Fig.10. Blue-stained aggregated yeasts in the neuropile; high fungal burden with mild to absent inflammatory infiltrate. Neurocryptococcosis, cerebellum, cat, Case 7. Alcian blue, obj.20x.

Yeast's morphology

The yeast cell, capsule thickness, and budding frequency are summarized in Table 4. Yeast cells ranged from round to oval and occasionally "sickle" shaped, with a mildly basophilic cytoplasm. They were surrounded by a mildly basophilic (and sometimes bi-refringent) cell wall, typically thin, and rapped by a large, clear capsule forming a distinct unstained halo in HE staining. The Alcian blue staining technique provided a more effective visualization of the capsules, highlighting their presence. Narrow-based buddings were occasionally observed in all cases (Fig.13). Chain budding was rare in Cases 6 and 9.

Increased cell wall thickness was observed in Cases 4, 7 and 8, wherein the wall was mildly eosinophilic and occasionally duplicated. Case 3 had a predominance of yeasts with absent to minimal capsule formation and decreased wall thickness; in all cases, yeasts with small capsules were usually seen inside the cytoplasm of macrophages, often in multinucleated giant cells or inside blood vessels (Fig.16). In areas with severe inflammatory infiltrate, there was frequent loss of the capsular architecture.

Yeasts in the lumen of blood vessels (vascular embolism) were occasionally observed in all cases, mostly within the meningeal vessels (Fig.16) and rarely in the neuropil vessels. Larger yeasts with thicker capsules were mainly visualized in the meninges (and lungs), or in large aggregates within the neuropil, usually associated with mild or absent inflammation.

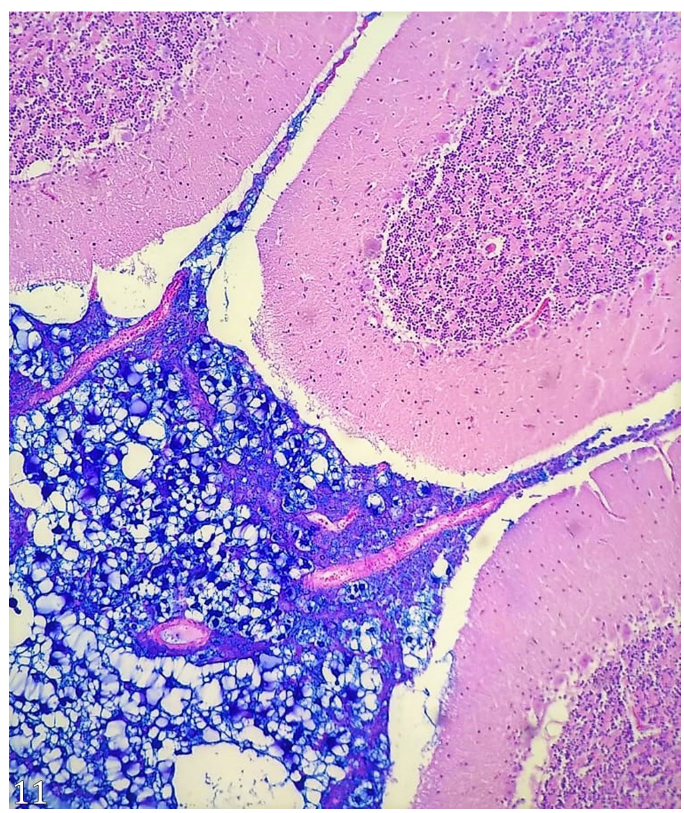

Fig.11. Blue-stained aggregated yeasts in the meninges forming large aggregates; high fungal burden with mild to absent inflammatory infiltrate. Neurocryptococcosis, cerebellum, cat, Case 6. Alcian blue, obj.20x.

Other affected organs

The upper respiratory tract lesions were observed in two cats (Cases 6 and 9), described as well-defined, round shapes with a grayish-to-whitish color and soft and gelatinous nodules. Microscopically, they were composed of aggregated yeasts with high fungal load infiltrated by mild inflammation of macrophages and lymphocytes. One cat (Case 9) had a nodule on the lateral region of the right nostril (measuring 2.0 x 1.5 x 1.0cm). The other cat (Case 6) had a nodule in the larynx (measuring 1.0 x 0.6 x 1.0cm). This animal also had a substantial amount of amorphous, soft, whitish material, occupying a significant portion of both frontal sinuses. Histopathology revealed a widespread presence of yeasts with mild to absent inflammatory infiltrate.

Histopathological examination of the lungs revealed the presence of yeasts in all cases; most had a low fungal burden (seven cases). However, in Cases 3 and 9, it was moderate, and in Cases 1 and 2, it was high. On gross examination, nine cases had lesions (all except Cases 3 and 4); the lungs appeared slightly firm, heavy, and shiny, occasionally with punctate areas of hemorrhage. Moderate to severe edema and congestion were frequently seen on histopathological examination, and yeasts were seen as individual or small groupings surrounded by a mild inflammatory infiltrate, predominantly composed of foamy macrophages. Yeast's cell enlargement was frequent in this organ, and there was a marked variation in size, from very small cells with minimal capsules to large cells surrounded by wider capsules.

Other organs where yeasts were detected included the lymph nodes (eight cases), spleen (four cases), skin (three cases), kidneys (three cases), liver, and heart (one case).

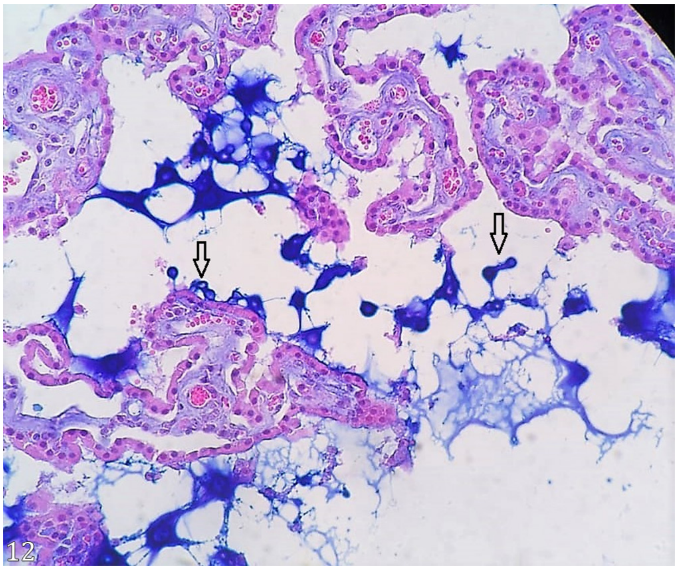

Fig.12. Blue-stained yeasts around choroid plexus blood vessels; severe fungal burden and mild inflammation. Indicate narrow-based budding and chain budding (arrows). Neurocryptococcosis, choroid plexus, cat, Case 6. Alcian blue, obj.40x.

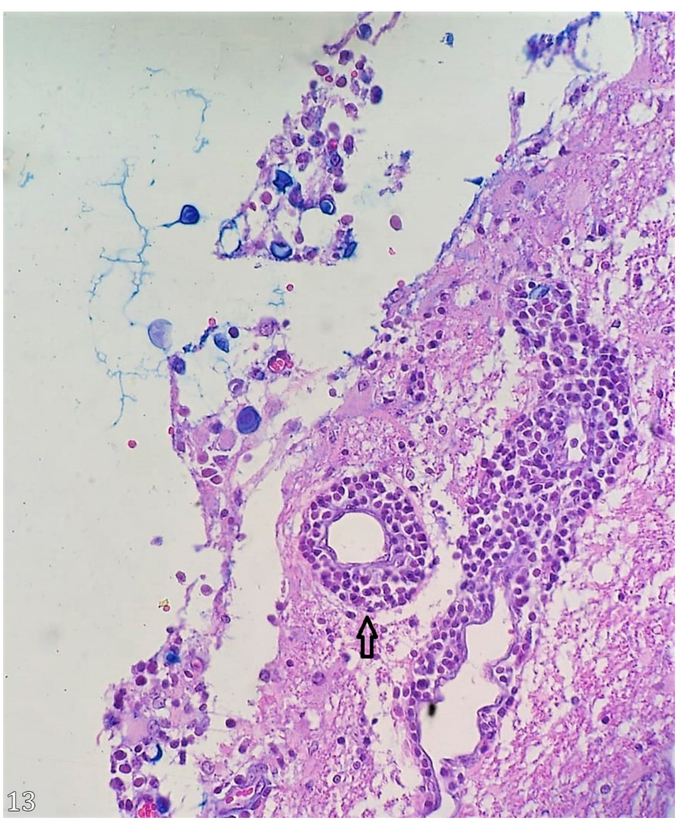

Fig.13. Blue-stained yeasts in the meninges, low fungal burden and moderate inflammation. Indicates accentuated perivascular lymphoplasmacytic inflammation (arrow). Neurocryptococcosis, telencephalic cortex, cat, Case 5. Alcian blue, obj.40x.

DISCUSSION

This case series comprises 11 small animals (nine cats and two dogs) with cryptococcosis, affecting, to some degree, the central and/or the peripheral nervous system. Neurological signs were observed in 54% of our cases (four cats and two

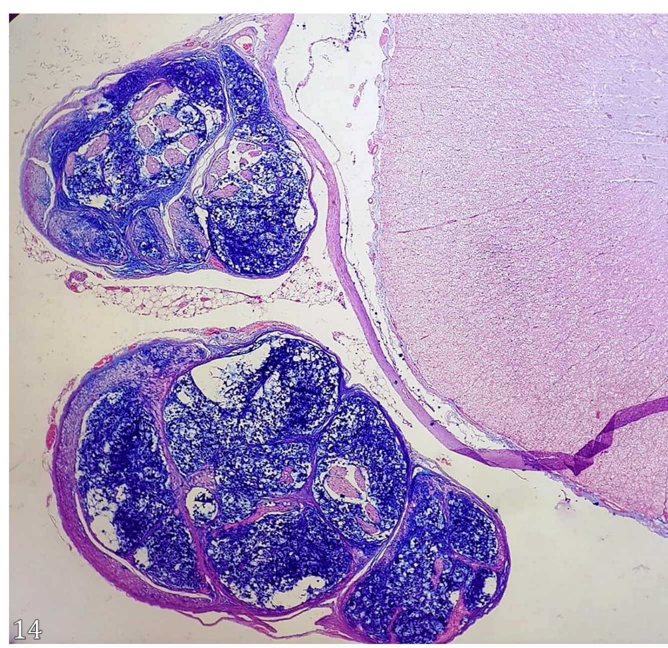

Fig.14. Blue-stained yeasts invading and partially replacing the nervous tissue, severe fungal burden with minimal inflammation. Neurocryptococcosis, spinal cord, nerve roots (lumbar region), dog, Case 11. Alcian blue, obj.10x.

dogs). Comparing these results to another study (Sykes et al. 2010), neurological signs were present in 95% of their animals. However, their cases were selected based on magnetic resonance imaging (MRI) findings. This difference can also be explained by the fact that not all animals in our study were neurological cases; many had only cutaneous or respiratory signs, but during the histopathological evaluation, they had lesions and yeasts in the nervous system.

The most common signs observed were blindness and head tilt. According to the literature, neurological signs usually include depression, circling, head pressing, paresis, lethargy, behavioral changes, gait abnormalities, vestibular signs (including head tilt), ocular signs consistent with nystagmus, tight circling, seizures, mydriasis, blindness (Caswell & Williams 2007). Apparent pain is more commonly reported in dogs (33%) than in cats (8%) in the cervical region and head (Sykes et al. 2010). In the present study, one dog (Case 11) had a clinical history of pain upon epaxial palpation throughout the vertebral column; the lesions observed on the nerve roots of the spinal cord, in this case, could provide an explanation for this pain.

Only three cases (cats, 27%) were clinically diagnosed with cryptococcosis before necropsy; all of these had cutaneous manifestations in this study. Cutaneous disease was seen in animals with neurocryptococcosis, being more common in cats (15%) than in dogs (4.7%) (Sykes et al. 2010). Small cutaneous or subcutaneous masses can aid in the clinical diagnosis, particularly in felines, where fungal rhinitis in the rostral nasal cavity is the most common presentation (Caswell & Williams 2007). The remaining eight cases (73%) had their definitive diagnosis after necropsy during histopathological examination in our study. A similar situation has been described by other authors in fungal infections, which describe a frequent lack of characteristic clinical alterations for a presumptive diagnosis (Kaufman 1992, Jensen et al. 1996, Sykes et al. 2010). When more accurate imaging analyses of the CNS were applied, such as magnetic resonance imaging (MRI) or computed tomography (CT scan), the clinical diagnosis of neurocryptococcosis showed improvement in one study (Sykes et al. 2010).

Table 4. Intensity of inflammation and fungal burden for each case (n=11)

Case	Capsule thickness	Wall thickness	Budding frequency
1	Regular**	Increased	Regular
2	Increased	Regular**	Regular
3	Decreased to absent	Decreased	High
4	Increased	Increased	High
5	Regular	Regular	Low
6	Regular	Regular	High
7	Increased	Increased	Low
8	Increased	Increased	High
9	Decreased	Decreased	High
10*	Regular	Regular	Low
11*	Regular	Regular	Low

* Cases of dogs, ** The thickness of the wall and the capsule were classified as decreased, regular, or increased subjectively compared to the parameters of Galiza et al. (2014).

In this study, it was tried to assess whether there was a pulmonary infection in all cases with neurocryptococcosis, considering that the agent lodges in the upper respiratory tract and then descends to the lungs, followed by secondary hematogenous spread to the CNS, eyes, skin, and other organs (Faria & Xavier 2009). In the routine of necropsies, the evaluation of the nasal cavity is not frequent unless there is an indication (such as skin lesions in the nasal area) for this evaluation. For this reason, in this study, pulmonary involvement was analyzed, as this organ is routinely examined, even in the absence of gross lesions or respiratory clinical signs. Only two

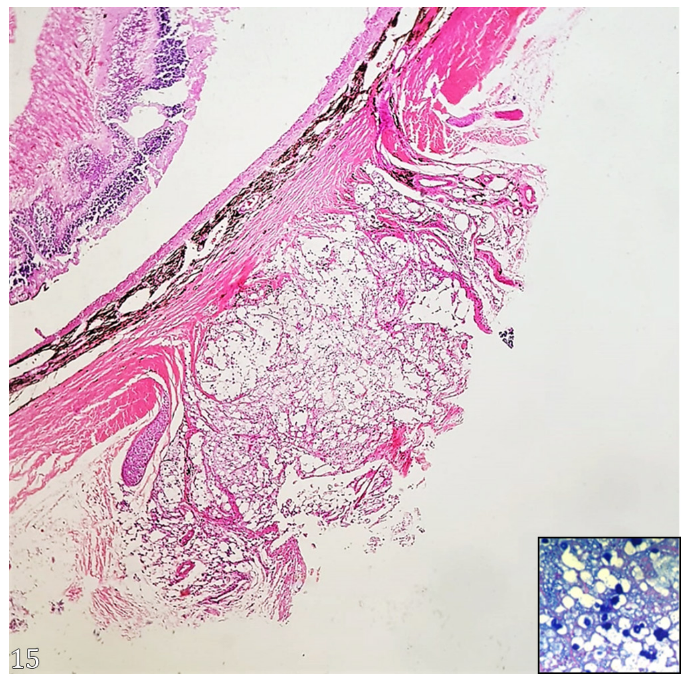

Fig.15. Invasion and replacement of the optic nerve region by yeasts. Neurocryptococcosis, eye, dog, Case 11. HE, obj.20x. Inset: Acian blue-stained yeasts in the optic nerve. Alcian blue, obj.20x.

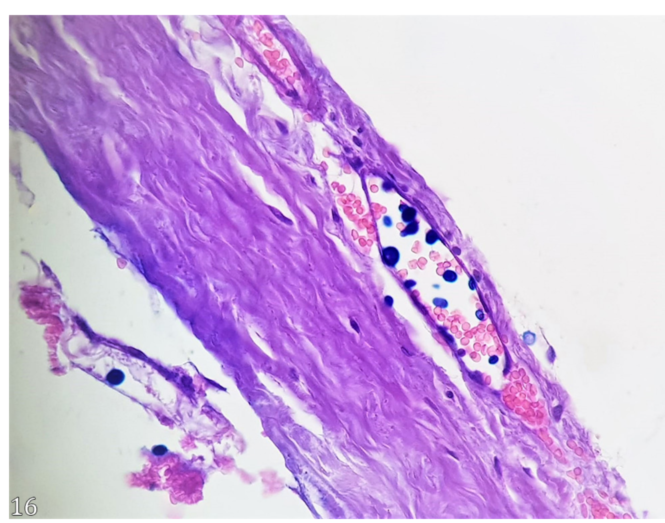

Fig.16. Blue-stained yeasts inside a blood vessel (fungal emboli) of the dura mater. Neurocryptococcosis, spinal cord (thoracic region), cat, Case 9. Alcian blue, obj.40x.

cases had nasal lesions; however, all the examined cases had pulmonary infection to some degree in this study.

Gross lesions found in the CNS were multiple small "cysts", referred to in the literature as "cryptococcomas", with a viscous, gelatinous appearance, being the faint gray appearance attributed to the presence of the mucinous capsule (Miller & Zachary 2016). Large gelatinous lesions, also referred to as "torulomas", indicating unrestricted growth of the cryptococcal organisms (Ristow & Davis 2021), could provide an explanation for Case 11 (dog) with a focally extensive enlarged area (measuring 11cm) in the lumbosacral region of the spinal cord, leading to the development of a significant lesion in that specific area. However, the reason for the involvement of that area was not determined in this case. Enlargement and softening of the olfactory bulbs and cerebellar herniation through the foramen magnum (11.5% each), as described in another study (Sykes et al. 2010), was not found in this case series. However, gray gelatinous masses (36%), opacity and congestion of the meninges, and foci of hemorrhage (9% each) were frequently observed in the CNS of our cases.

Despite the most common route the agent reaches the brain is through pulmonary infection, where the yeast spread through bloodstream through leukocytic trafficking (Caswell & Williams 2007), yeasts may also reach the brain through a different pathway, an infection (usually subclinical) of the nasal cavity, where the microorganism can quickly penetrate the nasal and frontal bones, reaching the brain by extension, either through the cribriform plate or optic nerves (Lester et al. 2004, Malik et al. 2006). In this study, lesions on the nasal cavity were detected in two cats; in one of them (Case 6), occupying a significant portion of both frontal sinuses. However, retrospectively, it was not possible to determine if the yeasts entered the CNS through the bloodstream or by extension since pulmonary involvement was present in this case.

The literature describes three histopathological patterns for neurological cryptococcosis in dogs and cats, which are not correlated with infecting species: a) pseudocyst formation, characterized by the expansion of cryptococcal organisms along ventricular and subarachnoid spaces, leading to random, multifocal, and variable-sized intraparenchymal pseudocysts; b) diffuse meningitis alone, without the presence of pseudocysts or involvement of the brain parenchyma; and c) meningoencephalitis without evident pseudocyst formation (Sykes et al. 2010). According to this classification, in our study, five cases (7, 11, 2, 4, 6) are compatible with the pseudocyst formation pattern (described in this case series as large aggregated yeasts inside the neuropile), three cases (10, 5, 9) with the diffuse meningitis alone pattern, and three cases (1, 3, 8) with the meningoencephalitis pattern.

In one cat (Case 5), no alterations were observed in the physical, hematological, and radiographic exams. However, histopathological examination of this case revealed a severe perivascular lymphoplasmacytic inflammation observed expanding the Virchow-Robin spaces. Yeasts were observed only in the meninges and the inflammatory infiltrate observed around them was distinctly different from the perivascular inflammatory infiltrate. A similar inflammatory infiltrate was seen, causing lymphoplasmacytic choroid plexitis and meningoencephalitis in a cat (Case 6). This phenomenon could have been caused by the translocation of yeasts from the bloodstream to the brain, leading to severe damage to the micro-vascular structure. The presence of rare yeasts associated with the vascular cuff in one of the cases supports this possibility (Charlier et al. 2005). Another possibility is that this animal could have a non-diagnosed concomitant viral disease (Pedersen et al. 2009).

The most affected neurolocations in our study were the telencephalic cortex and cerebellum (100% each), followed by the thalamus and hippocampus (72.7%) and pons (45.4%). Sykes et al. (2010) found similar CNS locations: Cerebrothalamic (96%), cerebellum (88%), pons and medulla (72%), and midbrain (52%). In one cat, the ependyma of the lateral ventricle showed infiltration by a mild number of yeasts. In a specific area, the yeasts were seen causing ependymal disruption; one case had the lateral ventricle markedly filled with yeasts. This finding may indicate the possibility of dissemination of the agent through the cerebrospinal fluid, corroborating the findings reported by other authors. Choroid plexitis was seen in one dog and two cats. These lesions are more often described in dogs with neurocryptococcosis (Sykes et al. 2010). In a study in mice (Charlier et al. 2005), yeast cells were not detected in the choroid plexus, a structure that consistently exhibited normal morphology.

In four cases (36%), yeasts were observed in the spinal cord, mostly in the leptomeninges and the subarachnoid and subdural spaces. Nerve root invasion was present in two cases (one dog and one cat). The paravertebral ganglia, however, were affected only in one cat; central canal or spinal cord parenchyma involvement was not observed. When comparing this to the literature, spinal cord involvement was observed in 18% of cats and 43% of dogs. Only one cat (9%) also had spinal nerve root involvement, and in 14% of the dogs, yeasts were seen in the central canal (Sykes et al. 2010).

The predominant yeast morphological pattern observed in this study was a central fungal cell surrounded by a thick (polysaccharide) capsule that typically did not stain with HE technique, giving the characteristic vacuolated appearance, often described as a "soap bubble" lesion (Malik et al. 2006, Faria & Xavier 2009, Kronstad et al. 2011). The capsule of the agent was strongly stained by Alcian blue. This staining proved to be an important tool in highlighting yeasts in tissues with very low fungal burden, as previously described (Galiza et al. 2014), particularly in the lungs, where the presence of yeasts was revealed in three cases (Cats 1, 5, and Dog 11) that were not previously detected by HE staining.

Only one cat (Case 3) displayed an aberrant morphological feature, where multiple tissues showed a predominance of yeasts with absent to minimal capsule formation, having rare yeasts with regular capsule sizes. This particular case stood out as the sole patient in this study with a previous history of treatment (drug not informed) for cryptococcosis. This morphological change may have a relation with the treatment since studies demonstrate that although individual treatment with Amphotericin B or TRB Terbinafine does not lead to a reduction in capsule, the combination of these two drugs significantly decreased capsule size compared to the control cells (Guerra et al. 2012).

In this case series, none of the cases had available information regarding the identification of *Cryptococcus* species via isolation/biochemical analysis or molecular typing, hindering the correlation with location, tissue reaction, and host condition. This fact probably reflects the frequent lack of macroscopic lesions that are suggestive of cryptococcosis, with adequate material not being collected for these evaluations during necropsy. However, it does not prevent the study of tissue damage caused by infection with this fungus genus, as demonstrated in a similar study of neurocryptococcosis (Sykes et al. 2010) on 11 cats and 14 dogs submitted to necropsy, in which only one cat (infected with *C. gattii)* and six dogs (four infected with *C. neoformans* and two with *C. gattii*) had the infecting *Cryptococcus* species determined.

The observed heterogeneity in the inflammatory response and fungal burden reveals the complex nature of this infection. Authors describe that it can be related to the yeast's virulence factors and the host's immunological status (Buchanan & Murphy 1998, Steenbergen & Casadevall 2003, Caswell & Williams 2007). However, further investigations are still needed to elucidate the implications of this variability, as well as to explore it for disease progression and management strategies, contributing to a better understanding of cryptococcosis pathogenesis.

CONCLUSION

This study shows the neuropathological features of cryptococcosis in a series of cases in dogs and cats, emphasizing the importance of considering specific neurolocations to diagnose this fungal infection. The telencephalic cortex and the cerebellum were consistently involved in all cases, along with the lungs, despite not all cases presenting neurological and/or respiratory signs or gross lesions in these tissues. These findings highlight the significance of necropsy and histopathologic examination as valuable diagnostic tools for cryptococcosis. Furthermore, these findings can guide critical areas when performing image analysis techniques on affected animals, improving diagnostic approaches for this condition.

Acknowledgments.- This research was financially supported by "Coordenação de Aperfeiçoamento de Pessoal de Nível Superior" (CAPES), Brazil - Finance code 001; M.D. Oliveira has a Master's scholarship from CAPES.

Conflict of interest statement.- The authors declare that there are no conflicts of interest.

REFERENCES

Baker R.P., Chrissian C., Stark R.E. & Casadevall A. 2022. Cryptococcus neoformans melanization incorporates multiple catecholamines to produce polytypic melanin. J. Biol. Chem. 298(1):101519. <https://dx.doi.org/10.1016/j.jbc.2021.101519> <PMid:34942148>

Bovers M., Hagen F. & Boekhout T. 2008. Diversity of the *Cryptococcus neoformans-Cryptococcus gattii* species complex. Revta Iberoamericana Micol. 25(1):4-12. <https://dx.doi.org/10.1016/s1130-1406(08)70019-6> <PMid:18338917>

Buchanan K.L. & Murphy J.W. 1998. What makes *Cryptococcus neoformans* a pathogen? Emerg. Infect. Dis. 4(1):71-83. <https://dx.doi.org/10.3201/eid0401.980109> <PMid:9452400>

Caswell L.J. & Williams K.J. 2007. Infectious diseases of the respiratory system, p.579-650. In Maxie M.G. (Ed.), Jubb, Kennedy and Palmer's Pathology of Domestic Animals. Vol.1. 5th ed. Elsevier, St. Louis.

Chang Y.C., Stins M.F., McCaffery M.J., Miller G.F., Pare D.R., Dam T., Paul-Satyaseela M., Kim K.S. & Kwon-Chung K.J. 2004. Cryptococcal yeast cells invade the central nervous system via transcellular penetration of the blood-brain barrier. Infect. Immun. 72(9):4985-4995. <https://dx.doi.org/10.1128/IAI.72.9.4985-4995.2004> <PMid:15321990>

Charlier C., Chrétien F., Baudrimont M., Mordelet E., Lortholary O. & Dromer F. 2005. Capsule structure changes associated with *Cryptococcus neoformans* crossing of the blood-brain barrier. Am. J. Pathol. 166(2):421-432. <https://dx.doi.org/10.1016/S0002-9440(10)62265-1> <PMid:15681826>

Eghwrudjakpor P.O. & Allison A.B. 2009. Neurocryptococcosis in a 10-year-old immunocompetent girl. Acta Neurochirurgica 151(6):711-712. <https://dx.doi.org/10.1007/s00701-009-0250-4> <PMid:19290466>

Faria N.R. & Xavier M.O. 2009. Criptococose, p.191-203. In: Cruz L.C.H. (Ed.), Micologia Veterinária. Ed. UFPel, Pelotas.

Galiza G.J.N., Silva T.M., Caprioli R.A., Tochetto C., Rosa F.B., Fighera R.A. & Kommers G.D. 2014. Características histomorfológicas e histoquímicas determinantes no diagnóstico da criptococose em animais de companhia. Pesq. Vet. Bras. 34(3):261-269. <https://dx.doi.org/10.1590/S0100-736X2014000300011>

Greene C.E. 2012. Infectious Diseases of the Dog and Cat. 4th ed. Elsevier Saunders, St. Louis. 1376p.

Guarner J. & Brandt M.E. 2011. Histopathologic diagnosis of fungal infections in the 21st century. Clin. Microbiol. Rev. 24(2):247-280. <https://dx.doi.org/10.1128/CMR.00053-10> <PMid:21482725>

Guerra C.R., Ishida K., Nucci M. & Rozental S. 2012. Terbinafine inhibits *Cryptococcus neoformans* growth and modulates fungal morphology. Mem. Inst. Oswaldo Cruz 107(5):582-590. <https://dx.doi.org/10.1590/S0074-02762012000500003> <PMid:22850947>

Guevara-Campos J., González-Guevara L., Urbáez-Cano J. & Fermín S. 2009. Meningoencefalitis por *Criptococcus neoformans* en escolares inmunocompetentes. Investig. Clín. 50(2):231-239. <PMid:19662818>

Hagen F., Khayhan K., Theelen B., Kolecka A., Polacheck I., Sionov E., Falk R., Parnmen S., Lumbsch H.T. & Boekhout T. 2015. Recognition of seven species in the *Cryptococcus gattii*/*Cryptococcus neoformans* species complex. Fungal Gen. Biol. 78:16-48. <https://dx.doi.org/10.1016/j.fgb.2015.02.009> <PMid:25721988>

Jensen H.E., Schønheyder H.C., Hotchi M. & Kaufman L. 1996. Diagnosis of systemic mycoses by specific immunohistochemical tests. Acta Pathol., Microbiol. Immunol. Scand. 104(4):241-258. <https://dx.doi.org/10.1111/j.1699-0463.1996.tb00714.x> <PMid:8645463>

Kaufman L. 1992. Immunohistologic diagnosis of systemic mycoses: an update. Eur. J. Epidemiol. 8(3):377-382. <https://dx.doi.org/10.1007/BF00158571> <PMid:1397200>

Kronstad J.W., Attarian R., Cadieux B., Choi J., D'Souza C.A., Griffiths E.J., Geddes J.M.H., Hu G., Jung W.H., Kretschmer M., Saikia S. & Wang J. 2011. Expanding fungal pathogenesis: *Cryptococcus* breaks out of the opportunistic box. Nature Rev. Microbiol. 9(3):193-203. <https://dx.doi.org/10.1038/nrmicro2522> <PMid:21326274>

Lacaz C.S., Porto E., Martins J.E.C., Heins-Vaccari E.M. & Takahashi de Melo N. 2002. Tratado de Micologia médica. 9ª ed. Sarvier, São Paulo. 1104p. <https://dx.doi.org/10.1590/S0036-46652002000500013>

Lester S.J., Kowalewich N.J., Bartlett K.H., Krockenberger M.B., Fairfax T.M. & Malik R. 2004. Clinicopathologic features of an unusual outbreak of cryptococcosis in dogs, cats, ferrets, and a bird: 38 cases (January to July 2003). J. Am. Vet. Med. Assoc. 225(11):1716-1722. <https://dx.doi.org/10.2460/javma.2004.225.1716> <PMid:15626222>

Malik R., Krockenberger M., O'Brien C.R., Martin P., Wigney D. & Medleau L. 2006. *Cryptococcus*, p.584-598. In: Greene C.E. (Ed.), Infectious Diseases of the Dog and Cat. 3rd ed. Saunders Elsevier, St. Louis.

Miller A.D. & Zachary J.F. 2016. Nervous system, p.841-843. In: Zachary J.F. (Ed.), Pathologic Basis of Veterinary Disease. 6th ed. Mosby, St. Louis.

Pinto L.I.S. 2010. A criptococose meníngea em doentes com infecção HIV. Tese de Mestrado, Universidade do Porto, Portugal. 25p.

Ristow L.C. & Davis J.M. 2021. The granuloma in cryptococcal disease. PLoS Pathog. 17(3):e1009342. <https://dx.doi.org/10.1371/journal.ppat.1009342> <PMid:33735307>

Seyedmousavi S., Bosco S.M.G., Hoog S., Ebel F., Elad D., Gomes R.R., Jacobsen I.D., Jensen H.E., Martel A., Mignon B., Pasmans F., Piecková E., Rodrigues A.M., Singh K., Vicente V.A., Wibbelt G., Wiederhold N.P. & Guillot J. 2018. Fungal infections in animals: A patchwork of different situations. Med. Mycol. 56(Supl.1):165-187. <https://dx.doi.org/10.1093/mmy/myx104> <PMid:29538732>

Steenbergen J.N. & Casadevall A. 2003. The origin and maintenance of virulence for the human pathogenic fungus *Cryptococcus neoformans*. Microbes Infect. 5(7):667-675. <https://dx.doi.org/10.1016/s1286-4579'03'00092-3> <PMid:12787743>

Summers B.A. 1995. Inflammatory diseases of the central nervous system, p.151-155. In: Cummings J.F. & Lahunta A. (Eds.), Veterinary Neuropathology. Mosby, St. Louis.

Sykes J.E. & Malik R. 2012. Cryptococcosis, p.621-634. In: Sykes J.E. & Greene C.E. (Eds), Greene Infectious Diseases of the Dog and Cat. 4th ed. Elsevier, St. Louis, Missouri.

Sykes J.E., Sturges B.K., Cannon M.S., Gericota B., Higgins R.J., Trivedi S.R., Dickinson P.J., Vernau K.M., Meyer W. & Wisner E.R. 2010. Clinical signs, imaging features, neuropathology, and outcome in cats and dogs with central nervous system cryptococcosis from California. J. Vet. Intern. Med. 24(6):1427-1438. <https://dx.doi.org/10.1111/j.1939-1676.2010.0633.x> <PMid:21054543>

Trivedi S.R., Sykes J.E., Cannon M.S., Wisner E.R., Meyer W., Sturges B.K., Dickinson P.J. & Johnson L.R. 2011. Clinical features and epidemiology of cryptococcosis in cats and dogs in California: 93 cases (1988-2010). J. Am. Vet. Med. Assoc. 239(3):357-369. <https://dx.doi.org/10.2460/javma.239.3.357> <PMid:21801050>

Williamson P.R., Wakamatsu K. & Ito S. 1998. Melanin biosynthesis in *Cryptococcus neoformans*. J. Bacteriol. 180(6):1570-1572. <https://dx.doi.org/10.1128/JB.180.6.1570-1572.1998> <PMid:9515929>